Available online at www.sciencedirect.com
SCIENCE DIRECT®
Journal of the Mechanics and Physics of Solids
53 (2005) 1855–1874
JOURNAL OF THE MECHANICS AND PHYSICS OF SOLIDS
www.elsevier.com/locate/jmps

Actuation of the Kagome Double-Layer Grid. Part 1: Prediction of performance of the perfect structure

D.D. Symons, R.G. Hutchinson, N.A. Fleck*

Cambridge University Engineering Department, Trumpington Street, Cambridge, CB2 1PZ, UK

Received 12 February 2004; accepted 23 February 2005

Abstract

The Kagome Double-Layer Grid (KDLG) is a sandwich-like structure, based on the planar Kagome pattern, which has properties that make it attractive for application as a morphing material. In order to understand the passive and active properties of the KDLG with rigid joints, an analysis is made of the determinacy of the pin-jointed version. The number of internal mechanisms and states of self-stress of the finite pin-jointed structure are calculated as a function of the size of the structure. A statically and kinematically determinate version is obtained by relocating the internal nodes and by prescribing a set of patch bars around the periphery. The actuation performance of the rigid-jointed version is then explored theoretically by replacing a single bar in the structure by an actuator. The resistance to actuation is determined in terms of the stiffness and the allowable actuation strain as dictated by yield and buckling. The paper concludes with the optimal design of a double-layer grid to maximise actuation performance.

Keywords: Buckling; Elastic–plastic material; Structures; Stability and bifurcation; Morphing structures

*Corresponding author. Tel.: +44 1223332650; fax: +44 1223765046.
E-mail address: naf1@eng.cam.ac.uk (N.A. Fleck).

0022-5096/$ - see front matter © 2005 Elsevier Ltd. All rights reserved.
doi:10.1016/j.jmps.2005.02.011

1. Introduction

There is increasing interest in the development of morphing materials which are stiff to external loads yet can undergo large changes of shape upon actuation by lengthening (or shortening) some part of the material. One strategy for identifying useful morphing materials is to consider periodic, pin-jointed trusses. If the *pin-jointed* structure is both kinematically determinate (no internal mechanisms) and statically determinate (no internal states of self-stress), it will be stiff under passive (i.e. static and external) loads, but will become a mechanism when any bar is actuated. It is anticipated that the rigid-jointed version of a statically and kinematically determinate pin-jointed structure will inherit a morphing capability. This approach is different from current methods of topology optimisation for morphing materials, see for example Bendsøe and Sigmund (2002). In the topology optimisation of morphing materials, the ideal topology of a compliant mechanism is generated by selective material placement in order to achieve an overall objective against a set of constraints. A systematic procedure for translating the compliant mechanism into an equivalent statically and kinematically determinate pin-jointed structure remains a research challenge.

The hunt for a periodic, statically and kinematically determinate 2D or 3D structure is a challenging task. Recently, Guest and Hutchinson (2003) have proved that no such infinite periodic structure exists. Hutchinson (2004) has shown, however, that the finite planar Kagome grid, with suitable patch bars on the periphery, is both statically and kinematically determinate, see Fig. 1a. In the present paper, we consider the finite Kagome Double-Layer Grid (KDLG) as shown in Fig. 1b, and we show that the pin-jointed version can be made to be both statically and kinematically determinate by perturbing the location of internal nodes and by prescribing a set of patch bars around the periphery. The double-layer grid can exist as a flat plate, or can be distorted into a shell-like structure with single or double curvature. We leave to a subsequent study the analysis of the fully 3D Kagome structure, with the microstructure of Tridymite.

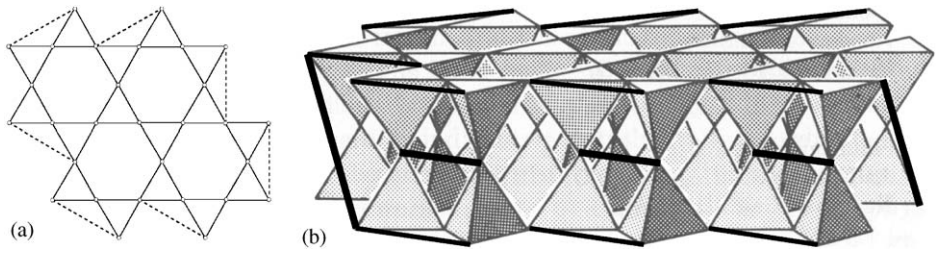

Fig. 1. (a) Finite "patched" planar Kagome grid and (b) topology of Kagome double-layer grid (KDLG) including patching scheme (faces of solid tetrahedra are absent in actual structure).

1.1. The planar Kagome truss

Consider the planar Kagome truss as sketched in Fig. 1a, with each truss bar made from a linear elastic solid of Young's modulus E_S. Hyun and Torquato (2002) have shown that the elastic, infinite version has in-plane effective properties which are close to optimal, and attains the upper Hashin–Shtrikman bound for a two-phase composite (where one phase is empty space). In the dilute limit, the in-plane Young's modulus E scales with the relative density of the cellular solid $\bar{\rho}$ according to

$$E = \tfrac{1}{3}\bar{\rho}E_S, \tag{1}$$

and the Poisson's ratio is $v = \frac{1}{3}$, see Hutchinson et al. (2003). Hutchinson (2004) has shown that the infinite pin-jointed structure has an infinite number of internal periodic collapse mechanisms, but none of these mechanisms produce macroscopic strain. This explains the paradox that the Kagome structure is stiff yet has internal collapse mechanisms.

1.2. The Kagome Double-Layer Grid

Two alternative "sandwich" constructions can be derived from the planar Kagome truss, as has been proposed by Hutchinson et al. (2003). One scheme is to attach a single planar Kagome truss to a solid plate via a tetrahedral core; such a structure has been considered by dos Santos et al. (2004). The second is the "KDLG", comprising two planar Kagome trusses and a double-layer tetrahedral core. The topology of the KDLG can be represented by an assembly of tetrahedra, with each tetrahedron defining the location of six neighbouring bars. In the actual structure, the faces of each tetrahedron do not exist: they are shown in Fig. 1b in order to help visualise the structure. The extensional stiffness and bending stiffness of the KDLG are high due to the fact that it behaves as a sandwich plate with planar Kagome grids as the faces. In this paper we explore the properties of the KDLG.

1.3. Outline of the study

The structure of the paper is as follows. First, linear algebra is used to investigate the properties of the finite pin-jointed KDLG. The number of internal mechanisms m and states of self-stress s is calculated as a function of the size of the structure. Second, a statically and kinematically determinate version is obtained by perturbing the location of internal nodes to thereby introduce asymmetry, and by prescribing a set of patch bars around the periphery. The actuation performance of the rigid-jointed version is explored by replacing a single bar by an actuator. The allowable actuation strain is dictated by yield and buckling of the KDLG. The paper concludes with a discussion of the effect of material properties and geometry upon actuation performance.

2. Determinacy of pin-jointed structures

It is envisaged that most practical realisations of the KDLG will have joints which have high rotational stiffness. However, the structural response can be informed by a consideration of the pin-jointed truss of identical topology. In this section, a matrix analysis is performed on pin-jointed, rigid-bar KDLG structures in order to explore whether internal mechanisms and states of self-stress exist. To achieve this the equilibrium (or equivalently the kinematic) matrix of the rigid, pin-jointed structure is analysed using the methodology of Calladine (1978), Pellegrino and Calladine (1986) and Pellegrino (1993). The fundamental set of subspaces of the equilibrium matrix is obtained by a singular value decomposition procedure, implemented within the software package MATLAB (2002). These subspaces provide the states of self-stress and internal mechanisms.

2.1. Search for a statically and kinematically determinate KDLG

Maxwell's equation, as modified by Calladine (1978), for a finite pin-jointed truss of b bars and j joints is

$$s - m = b + c - dj, \tag{2}$$

where s is the number of states of self-stress, m the number of mechanisms, c the number of constraints in the structure and d is the dimension of the problem (2 for a planar structure, and 3 for a 3D lattice). A statically and kinematically determinate structure has the property that $s = m = 0$, and we seek such a structure as the ideal topology for a morphing material.

The finite KDLG has a reduced connectivity at the periphery giving rise to mechanisms $m > 0$. Additional boundary bars can be added to remove these mechanisms; we refer to the finite structure with these additional bars as "patched".

But there remains a problem. Both the unpatched and patched KDLG possesses $s > 0$ due to its symmetry about the mid-plane. This symmetry can be broken by moving the joints of the mid-plane: the resulting KDLG is referred to as "asymmetric". For consistency, the KDLG is referred to as "symmetric" when it is symmetric about the mid-plane. We shall show that an asymmetric, patched KDLG gives us $s = m = 0$.

2.2. Symmetric structure

2.2.1. States of self-stress

Matrix analysis of "symmetric" KDLGs reveals that states of self-stress exist ($s > 0$) for KDLGs containing a sufficiently large number of bars. States of self-stress are combinations of bar tensions that are in equilibrium with zero external loads. Such states of self-stress are undesirable for a morphing structure as they may be excited by the extension of any bar in the structure, thereby producing a high resistance to bar actuation.

The "7-hexagon" structure is the smallest symmetric KDLG that contains a state of self-stress ($s = 1$). The name "7-hexagon" indicates the number of whole hexagons visible in a plan view of the grid, and this structure with its attendant state of self-stress is shown in Fig. 2a. The colours indicate the magnitude of the axial force within each bar according to the legend. Absolute values are arbitrary, but the magnitude of the vector of bar forces has been normalised to give a maximum value of unity.

A singular value decomposition of the equilibrium matrix of the symmetric KDLG structure reveals that each state of self-stress has a mechanism associated with it. Each mechanism involves equal and opposite out-of-plane displacements of adjacent nodes on the faces of the KDLG, as sketched in Fig. 2b. These mechanisms of the pin-jointed truss are reflected by unwanted compliant modes of deformation in the rigid-joint configuration.

Consider a plan view of a KDLG with n hexagons per side, see Fig. 3. The total number of hexagons H in a plan view of the double-layer grid is

$$H = 3n^2 - 3n + 1. \tag{3}$$

The $H = 7$ structure ($n = 2$) contains a single state of self-stress. Larger structures contain additional states of self-stress; the number of these states equals the number of 7-hexagon units contained within the structure. A simple formula can thereby be derived, such that the number of states of self-stress for a KDLG comprising n hexagons per side is

$$s = 3n^2 - 9n + 7 \quad \text{for } n > 1. \tag{4}$$

These relationships are plotted in Fig. 3. The implication is that larger, symmetric, KDLG structures provide increasing resistance to actuation and will therefore be increasingly less suitable for actuation.

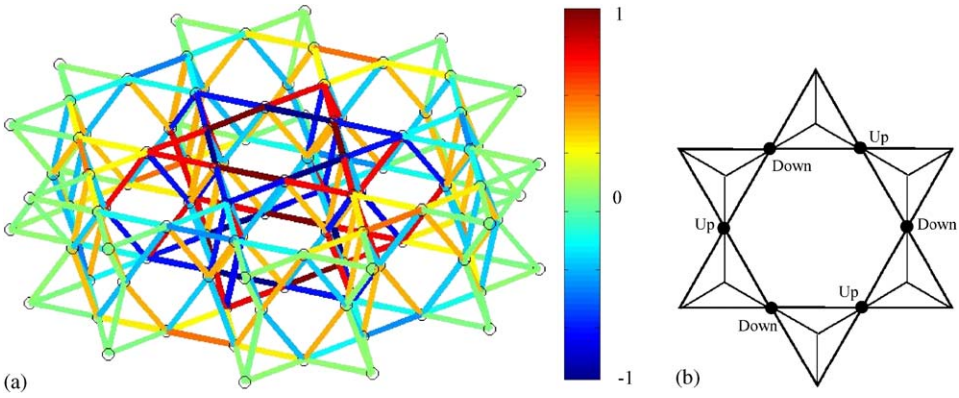

Fig. 2. (a) State of self-stress in symmetric 7-hexagon KDLG and (b) complementary mechanism in a symmetric KDLG.

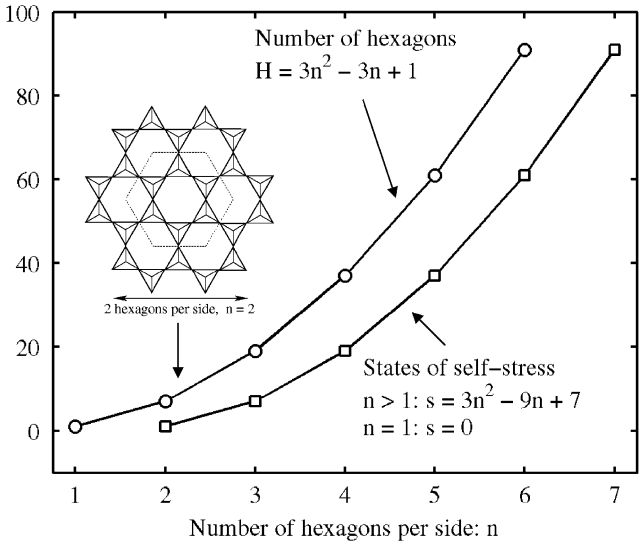

Fig. 3. Number of hexagons and states of self-stress in symmetric KDLG topologies.

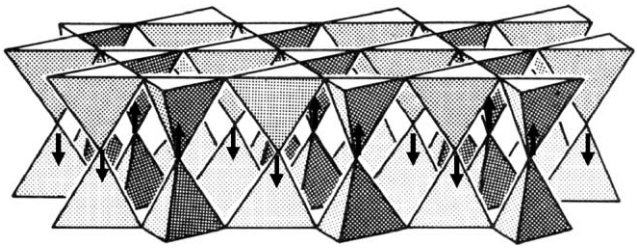

Fig. 4. Modification scheme for the asymmetric KDLG.

2.3. Asymmetric structure

The "symmetric" pin-jointed KDLG contains both states of self-stress and mechanisms. Consequently, it is not an ideal morphing material. Numerical experimentation using matrix analysis of the pin-jointed KDLG reveals that breaking the mid-plane symmetry of the KDLG removes the states of self-stress (and also removes the complementary mechanisms). This is done by moving the mid-plane nodes alternately up and down to produce an "asymmetric" KDLG, as illustrated in Fig. 4. This sequence of nodal re-positioning has the distinct advantage that it gives rise to a core which can be fabricated by folding.

2.4. Patching scheme

The finite asymmetric KDLG contains no states of self-stress ($s = 0$) and is therefore statically determinate. To make the structure kinematically determinate

($m = 0$) the remaining mechanisms must be "switched off" by a peripheral patching scheme.

We consider first a planar Kagome grid of n hexagons per side, and derive the required patching scheme. This grid contains $6n^2$ triangles, $b = 18n^2$ bars, and $j = 9n^2 + 3n$ joints. Recall that the finite, planar Kagome grid contains no states of self-stress, $s = 0$. Upon applying three constraints, $c = 3$, to prevent rigid body motions, the number of mechanisms (and therefore the number of required patch bars) follows from the 2D version of Maxwell's equation

$$s - m = b + c - 2j \tag{5}$$

giving

$$m = 6n - 3. \tag{6}$$

Thus, for the planar 7-hexagon Kagome grid ($n = 2$) we require nine patch bars. There remains an arbitrary choice in the location of the patch bars, but the arrangement shown in Fig. 1a is systematic and straightforward to generate.

The same approach is used to obtain the required number of patch bars for the 3D KDLG. A KDLG with faces containing n hexagons per side has a total of $12n^2$ tetrahedra and therefore the number of bars is

$$b = 72n^2. \tag{7}$$

The number of joints is

$$j = 24n^2 + 6n. \tag{8}$$

If we apply 6 constraints ($c = 6$), to prevent rigid body motions the 3D form of Maxwell's equation

$$s - m = b + c - 3j \tag{9}$$

implies

$$m - s = 18n - 6. \tag{10}$$

For the asymmetric KDLG, we have $s = 0$ and therefore the required number of patch-bars is $18n - 6$. The associated patching scheme is sketched in Fig. 1b. The scheme for the top and bottom faces and the mid-plane nodes closely resembles that sketched in Fig. 1a for the planar Kagome grid. Three additional patch bars complete the patching scheme and these bars connect the top and bottom layers of the KDLG.

2.5. Case study: the 7-hexagon KDLG

Consider the 7-hexagon KDLG; as noted above, this is the smallest KDLG which can contain a state of self-stress. The number of states of self-stress s and mechanisms m have been calculated for the patched and unpatched KDLG in both its symmetric and asymmetric forms. The results for the four topologies are summarised in Table 1.

Table 1
Comparison of the four versions of the 7-hexagon KDLG, $H = 7$, $n = 2$

Topology	b	c	j	s	m
Symmetric, no patches	288	6	108	1	31
Symmetric, patched	318	6	108	6	6
Asymmetric, no patches	288	6	108	0	30
Asymmetric, patched	318	6	108	0	0

The 7-hexagon unpatched KDLG comprises 48 tetrahedra, 288 bars, and 108 joints, as listed in Table 1. Now invoke Maxwell's equation, $s - m = b + c - 3j$, with six constraints ($c = 6$) to remove all rigid body motions. We are left with $s - m = -30$ for both the symmetric and asymmetric geometries. A calculation of the rank of the equilibrium matrix gives $(s = 1, m = 31)$ for the symmetric unpatched structure, and $(s = 0, m = 30)$ for the asymmetric unpatched KDLG.

Now add 30 patch bars (nine for each of the top, mid- and bottom planes, plus an additional three) in an attempt to remove 30 mechanisms, and thereby give $s - m = 0$. A calculation of the rank of the equilibrium matrix gives $s = m = 6$ for the symmetric patched structure which means that we have not been successful in eliminating all internal mechanisms; in fact the symmetry is such that we have introduced six additional states of self-stress. However, our attempt is successful in the asymmetric case and $s = m = 0$ for the asymmetric patched KDLG. It is concluded that only the asymmetric patched KDLG is statically and kinematically determinate.

3. Methodology for calculating the actuation properties of KDLG

Consider the replacement of any rigid bar in a statically and kinematically determinate pin-jointed structure by an axial actuator; the structure behaves as a mechanism with a single degree of freedom upon activation of the actuator. The mechanism involves extension of the actuator with all other bars remaining fixed in length. A matrix analysis of the pin-jointed structure will give the nodal displacements associated with this mechanism, see Pellegrino (1993). We shall address below the practical case of actuation of KDLGs with rigid joints.[1] Actuation is resisted by elastic bending and stretching of the remaining passive bars and is limited by the onset of yield or elastic buckling at sufficiently large actuator displacements.

The relative contributions of stretching and flexural stiffness in a rigid-jointed truss depend upon the stockiness S of the constituent bars. Here, stockiness is

[1]In Part II of this study (Symons et al., 2004) KDLG have been manufactured by sheet metal forming and brazing. The face sheets are computer-numerical control (CNC) laser-cut from mild steel sheet, the core sheets are laser-cut and folded from mild steel sheet to form the double-layer tetrahedral core, and the entire assembly is then spot welded or brazed together.

defined as the ratio of the radius of gyration λ to the length L of the bar

$$S = \lambda/L \tag{11}$$

with the second moment of area I of the bar related to its cross-sectional area A by

$$I = A\lambda^2. \tag{12}$$

The actuation stiffness, first yield load and elastic buckling load of rigid-jointed KDLGs are quantified below using a p-version of the finite element method, as implemented in the commercial software package Pro/Mechanica (PTC, 2001). This program is limited to linear, elastic behaviour. Theoretical foundations of the p-method are discussed by Babuska et al. (1981) and Babuska and Szabo (1982). The constituent lattice members of the KDLG are treated as Timoshenko (shear flexible) beams while the joints are treated as rigid, but of vanishing volume. Each bar is represented by a single variable-order element, and is considered to have a circular cross-section with a Poisson's ratio of 0.3.

Additional finite element calculations of the non-linear elastic–plastic response have been performed using the finite element program ABAQUS/Standard (HKS, 2003). The simulations used non-linear kinematics and the structures were discretised into five Euler–Bernoulli cubic order beam elements per bar.

In the simulations, the actuated bar is replaced by a slider mechanism which is rigid to shear and bending, but possesses zero axial stiffness. The slider is extended and the resistive force of the structure is determined in order to define the *actuation stiffness*. In addition, we calculate the actuator force for the onset of yield or buckling of any member, assuming linear elastic behaviour.

4. Actuation stiffness

4.1. Effect of size of structure upon the actuation stiffness of symmetric, unpatched KDLGs

Consider first the actuation of a symmetric, unpatched KDLG with rigid joints. In its pin-jointed form, this structure has an increasing number of states of self-stress with increasing size. Fig. 5a shows a plan view of five such structures. We investigate the actuation stiffness of each structure by replacing a single, central, bar in the bottom layer of the KDLG (as shown in bold in Fig. 5a) by a slider mechanism. The resistive force provided by the KDLG is calculated using the finite element program Pro/Mechanica. Displacement constraints are applied to three nodes adjacent to the actuated bar (as shown in Fig. 5a) in order to prevent rigid body motion.

The actuation stiffness k of the symmetric KDLG structures is plotted in the non-dimensional form kL/EA as a function of stockiness S of each member in Fig. 5b. The group kL/EA denotes the ratio of the passive stiffness k of the restraining structure to the axial stiffness EA/L of an individual bar. It is evident from Fig. 5b that the actuation stiffness of the 6-hexagon structure scales as S^2: this implies that the actuation stiffness is dictated by bending of the members. This is consistent with

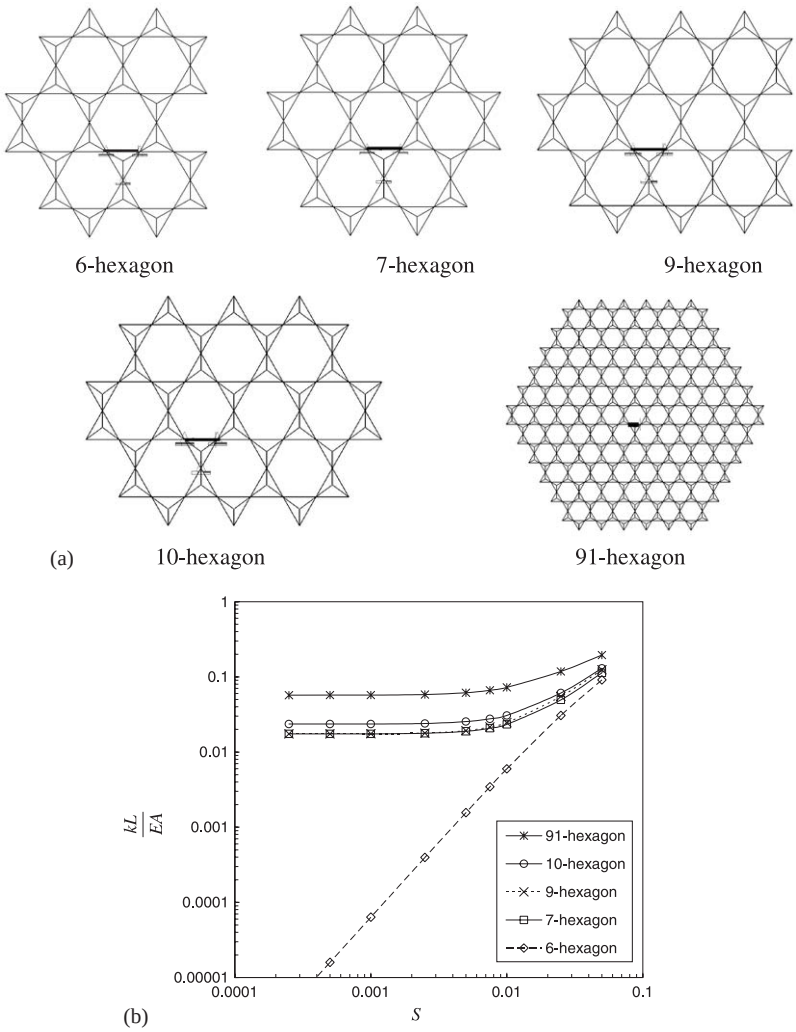

Fig. 5. (a) Plan views and (b) actuation stiffness of various symmetric, unpatched, rigid-jointed KDLG structures.

the fact that the pin-jointed version of the 6-hexagon KDLG has no states of self-stress. In contrast, the pin-jointed 7-hexagon structure has a single state of self-stress; consequently, the rigid-jointed version is stretching dominated and displays a constant value of kL/EA over a wide range of values of S.

An increase in size of the structure from 7-hexagon to 9-hexagon has very little effect upon the stiffness because no additional state of self-stress is introduced in the pin-jointed version. The 10-hexagon pin-jointed structure, however, has two states of self-stress and this endows the rigid-jointed version with a higher actuation stiffness. The trend of increasing stiffness with increasing number of states of self-stress in the

parent pin-jointed structure continues: Fig. 5b shows that a 91-hexagon structure, with 61 states of self-stress, has the highest actuation stiffness.

4.2. Effect of the degree of asymmetry upon the actuation stiffness of unpatched KDLGs

It has been shown above that the states of self-stress in the symmetric pin-jointed KDLG may be removed by moving the mid-plane nodes off the mid-plane. We now investigate the effect of this asymmetry upon the actuation stiffness of an unpatched KDLG.

Consider the smallest unpatched KDLG that, in pin-jointed form, contains a single state of self-stress. This is the 7-hexagon structure. In order to explore the effect of size of asymmetric nodal displacement upon the actuation stiffness we consider the 7-hexagon, rigid-jointed KDLG in four states: symmetric, and asymmetric with a 1%, 5% and 15% asymmetry. The magnitude of asymmetry is the out-of-plane displacement of the mid-plane nodes normalised by the total thickness of the KDLG (that is, normalised by the distance between the two planar Kagome grids). For each of these four structures, the non-dimensional actuation stiffness kL/EA is plotted against stockiness S in Fig. 6.

The normalised actuation stiffness of the symmetric KDLG is almost insensitive to bar stockiness. Its behaviour is stretching controlled because of the state of self-stress in the pin-jointed version. In contrast, the 15% modified structure is bending controlled and its normalised actuation stiffness scales with S^2. This is consistent with the fact that the state of self-stress in the pin-jointed version of the structure has been removed. The behaviour of the 1% and 5% modified structures is more

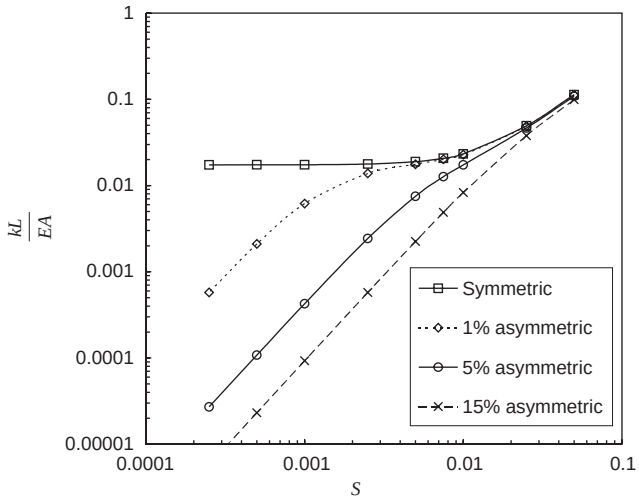

Fig. 6. Actuation stiffness of 7-hexagon, unpatched, KDLG structures with increasing asymmetry of mid-plane node position.

complex. At small values of S, the mode of deformation extends to the periphery of the structure and the actuation stiffness scales as S^2. However, for large values of S the actuation mode is local to the actuator, as discussed in the 2D planar case by Wicks and Guest (2004), and the actuation stiffness scales with S. In this regime, the contributions of axial and bending stiffness to the actuation stiffness become approximately equal.

4.3. *Effect of patch bars and asymmetry upon the actuation stiffness of KDLGs*

Recall that the finite, asymmetric, pin-jointed KDLG requires peripheral patch bars in order to make it kinematically determinate (no mechanisms). We shall now investigate the behaviour of rigid-jointed KDLGs in patched and unpatched, and symmetric and asymmetric realisations. The non-dimensional actuation stiffness of five prototypical structures is plotted in Fig. 7 as a function of bar stockiness.

The five structures are:

1. 91-hexagon, symmetric, patched KDLG, designated *91hex-S-P*,
2. 91-hexagon, symmetric, unpatched KDLG, designated *91hex-S-U*,
3. 91-hexagon, 15% asymmetric, patched KDLG, designated *91hex-15%-P*,
4. 91-hexagon, 15% asymmetric, unpatched KDLG, designated *91hex-15%-U*,
5. 7-hexagon, 15% asymmetric, patched KDLG, designated *7hex-15%-P*,

A consideration of these five structures allows us to investigate the effect of asymmetry, patching and size of structure upon the actuation stiffness. The 91-hexagon arrangement has been selected as being sufficiently large to find practical application.

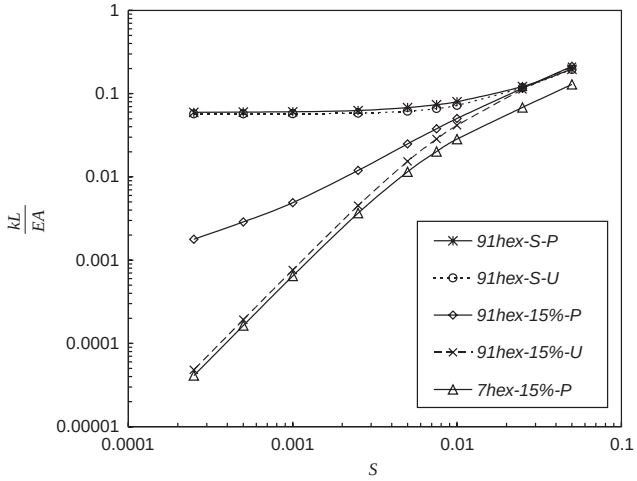

Fig. 7. Non-dimensional actuation stiffness of five KDLGs.

The *7hex-15%-P* KDLG is derived from a statically determinate pin-jointed structure and has an attractively low actuation stiffness, see Fig. 7. The actuation mode involves bending of the members and this gives rise to a quadratic dependence of kL/EA upon S. This is reminiscent of the actuation of a regular 2D-hexagonal rigid-jointed framework as analysed by Wicks and Guest (2004).

The *91hex-15%-P* KDLG has a significantly higher actuation stiffness than the *7hex-15%-P* case. Here, actuation primarily involves bending of members in a boundary layer surrounding the actuated member. Remote from the actuator the displacement field is dictated by stretching of the members. This competition between local bending and remote stretching gives rise to a characteristic decay length within the structure. Wicks and Guest (2004) have studied this in some detail for a 2D Kagome structure. A consequence is that kL/EA scales linearly with S, see Fig. 7. Note that the peripheral patch on the 91-hexagon asymmetric structure is needed in order for the outer bars to be stretching dominated. Without the patch (*91hex-15%-U*), the structure is bending dominated and kL/EA scales with S^2.

Now consider the symmetric 91-hexagon KDLG (both *91hex-S-P* and *91hex-S-U*). The 61 states of self-stress in the pin-jointed version leads to the rigid-jointed variants behaving in a stretching manner with or without the patch. Consequently $kL/EA \approx 0.1$ and the structure has a high resistance to actuation.

It is concluded that the 91-hexagon, 15% asymmetric, patched KDLG (*91hex-15%-P*) is the version which is most likely to find practical applications: its actuation stiffness is small, particularly at low values of stockiness S. It is demonstrated below that this structure also has an acceptable value of actuation strain before it buckles elastically or yields plastically. It is instructive to plot the out-of-plane deflected shape of the *91hex-15%-P* KDLG, see Fig. 8. The contour plots give the out-of-plane deflection of the top and bottom surfaces of the grid, for unit extension of the single central actuator. The amplitude of deflection and the spatial extent of the deflection zone both decrease with increasing bar stockiness S: compare the contour plot for

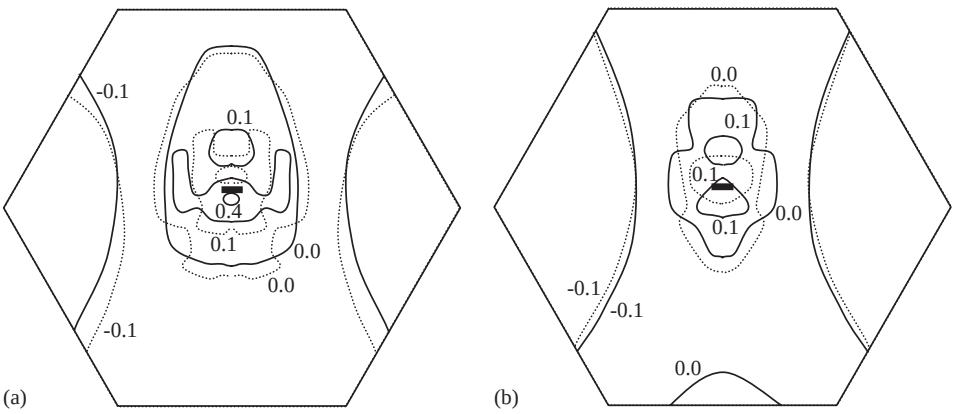

Fig. 8. Contour plots of out-of-plane displacement of top (solid) and bottom (dotted) surfaces of *91-hex-15%-P* KDLG for unit extension of a single central bar: (a) $S = 0.007$ and (b) $S = 0.25$.

$S = 0.007$ in Fig. 8a with the case $S = 0.25$ in Fig. 8b. We note in passing that the lower face of the plate deflects in similar manner to the top face, and the mode of deflection can be approximated to that of an ovalised blister.

5. Actuation limits of Kagome Double-Layer Grids

We now investigate the actuation limit for each of the KDLG structures considered above. Actuation is limited either by elastic buckling or by the onset of yield of the structure. (The fatigue strength of a repeatedly actuated structure scales with the load for first yield, although an additional knock-down factor is required.) In the following sections, the achievable actuation load and actuation strain are determined as a function of stockiness of each KDLG. Attention is focused on the most promising morphing material in the form of the 91-hexagon asymmetric, patched structure (*91hex-15%-P*). The sensitivity of achievable actuation strain to material choice and to the shape of cross-section is then addressed.

5.1. Elastic buckling

The lowest actuation buckling load P_b for each KDLG is calculated using the program Pro/Mechanica (2001) for the five structures detailed in Section 4.3 and with stiffness response shown in Fig. 7. We anticipate that the buckling load is sensitive to the stockiness of all bars including the patch bars; in this study we make the arbitrary choice that all patch bars have the same stockiness as internal bars. It is instructive to normalise P_b by the Euler buckling load P_E for a pin-jointed strut of the same cross-sectional area and stockiness as that of the parent KDLG structure, $P_E \equiv \pi^2 EI/L^2 = \pi^2 EAS^2$. It is found that the normalised buckling load P_b/P_E for the five structures is only mildly sensitive to the magnitude of the stockiness S and lies within the range of 1.2–4.1 for values of S between 0.00025 and 0.05. No weak long-wavelength modes exist, and all structures investigated can bear a buckling load in excess of the Euler load for a pin-jointed strut. This makes all of the structures promising for carrying high actuation loads.

The actuation strain at buckling ε_b is related to the buckling load P_b of the actuated structure by

$$\varepsilon_b = \frac{P_b}{kL}, \tag{13}$$

where the actuation stiffness k has already been introduced. The actuation buckling strain for the five structures is plotted against S in Fig. 9a. The symmetric KDLGs (*91hex-S-P* and *91hex-S-U*) are stretching dominated. Thus the buckling strain scales with S^2. In contrast, the *7hex-15%-P* and *91hex-15%-U* are bending-dominated structures and have actuation stiffnesses which scale with S^2 (see Fig. 7); consequently, the buckling strain is insensitive to S at low values of S. The *91hex-15%-P* KDLG shows intermediate behaviour due to the interaction of stretching and bending within it.

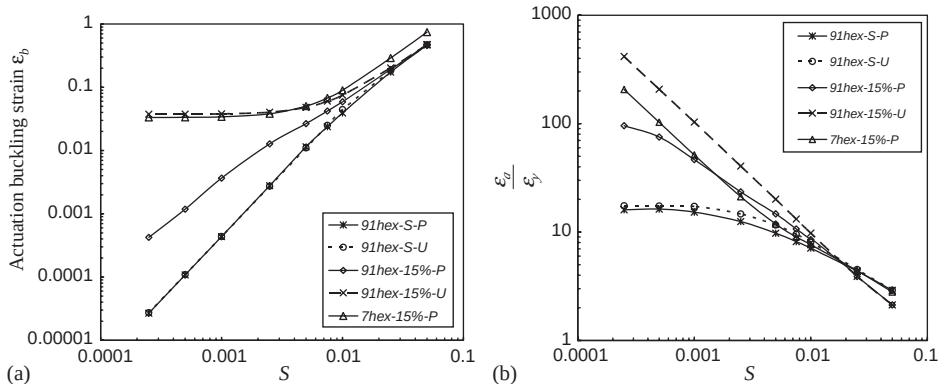

Fig. 9. (a) Actuation strain of five KDLGs limited by buckling and (b) by first yield.

5.2. Onset of yield

Potential failure modes for a morphing structure include the onset of yield and fatigue failure. Consequently, strains should be kept within the elastic limit of the structure. The actuation load for the onset of first yield of any member P_y has been calculated using Pro/Mechanica (2001) for each of the five structures described in Section 4.3. In general, first yield initiates in a single bar at a joint adjacent to the actuator.

The actuation strain at first yield ε_a is given by

$$\varepsilon_a = \frac{P_y}{kL}. \tag{14}$$

It is instructive to normalise ε_a by the material yield strain ε_y and to plot the normalised values against S, see Fig. 9b. The relative ranking of the five structures by the metric $\varepsilon_a/\varepsilon_y$ is the reverse of that noted in Fig. 7 for the normalised actuation stiffness kL/EA. This is due to the extreme sensitivity of actuation stiffness k to the type of structure. At low stockiness, $S<0.001$, the achievable actuation strain for the stretching structures (*91hex-S-P* and *91hex-S-U*) is about 20 times ε_y. In contrast, for the bending structures, ε_a is two to three orders of magnitude that of ε_y. The ratio $\varepsilon_a/\varepsilon_y$ decreases monotonically with increasing S in all cases, and converges to $\varepsilon_a/\varepsilon_y = 1$ as S approaches about 0.3.

6. Optimal actuation strain

Yield and buckling are competing failure mechanisms, with yield dominating at high stockiness and buckling dominating for slender bars. The maximum possible actuation strain is achieved where the two failure modes coincide. It is of practical significance to explore how the achievable actuation strain can be maximised. Consider two strategies: changing the material and changing the shape of the bar

cross-section. We restrict the discussion to the practical case of the 91-hexagon, 15% asymmetric, patched KDLG (*91hex-15%-P*).

6.1. Effect of yield strain upon achievable actuation strain

The magnitude of the yield strain ε_y of the constituent bars has no effect upon the actuation strain for buckling ε_b. In contrast, the actuation strain for yield ε_a is directly proportional to ε_y and consequently the choice of material has a direct effect upon the achievable actuation strain. The actuation limit for yielding ε_a of the *91hex-15%-P* structure is plotted against S in Fig. 10a for the choices $\varepsilon_y = 0.1\%$, 0.3% and 1%. The figure includes the dependence of the buckling strain ε_b upon S. For a solid with $\varepsilon_y = 0.1\%$ the optimum stockiness is $S = 0.0035$ and the maximum actuation strain is only 1.8%. However, an increase in the value of ε_y to 1% leads to a maximum actuation strain of 7.5% at $S = 0.012$. We now investigate the non-linear behaviour of the KDLG at selected values of stockiness for a choice of yield strain

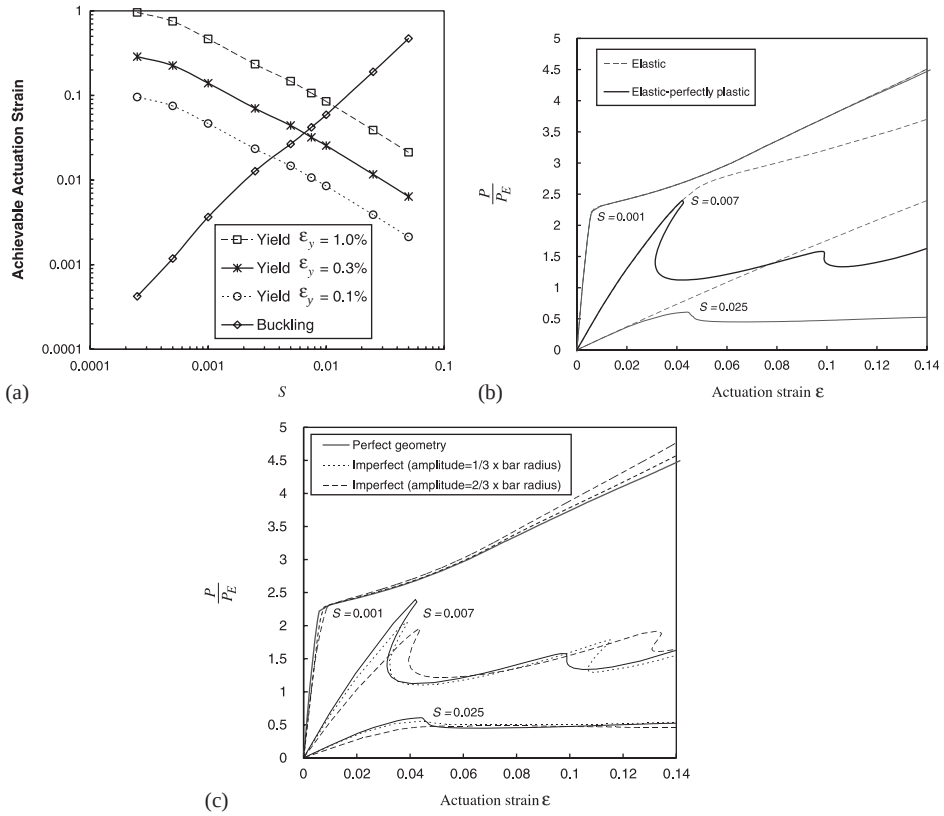

Fig. 10. (a) Achievable actuation strain for *91-hex-15%-P* KDLG limited by buckling or yield (for $\varepsilon_y = 0.1\%$, 0.3% and 1%), (b) elastic and elastic–plastic and (c) perfect and imperfect, load versus strain responses for *91-hex-15%-P* KDLGs of variable stockiness ($S = 0.001, 0.007$ and 0.025) with $\varepsilon_y = 0.3\%$.

(0.3%) which is representative of that for a medium strength alloy of steel, aluminium or titanium.

6.2. Post-buckling and yield response

The post-buckling and post-yield response of KDLG structures has been calculated using the ABAQUS/Standard (HKS, 2003) non-linear finite element software. Typical load displacement responses are shown in Fig. 10b. The simulations assume non-linear kinematics, and each bar is represented by five Euler–Bernoulli cubic beam elements. The assumed material response is either elastic, or elastic–perfectly plastic with a yield strain $\varepsilon_y = 0.3\%$.

Fig. 10b shows the actuation load versus strain response of the *91hex-15%-P* KDLG with selected values of stockiness ($S = 0.001, 0.007$ and 0.025). These values of S represent a slender, optimal and stocky KDLG, respectively, for the choice $\varepsilon_y = 0.3\%$. The actuation force P has been non-dimensionalised by the Euler buckling load P_E of a single pin-jointed strut of the same cross-sectional area and stockiness as that of the parent KDLG structure. The plot includes predictions for both elastic and elastic–perfectly plastic material responses.

The slender KDLG ($S = 0.001$) buckles elastically at an actuation strain of 0.004, and the post-buckling response remains elastic up to a large value of actuation strain of 0.1. In contrast, the stocky KDLG ($S = 0.025$) yields rather than buckles at an actuation strain of $\varepsilon_a \approx 3.9\varepsilon_y = 0.012$. The KDLG with optimal stockiness ($S = 0.007$) undergoes simultaneous elastic buckling and yield at an actuation strain of 0.04. It is anticipated that the coincidence of failure modes will make the structure imperfection sensitive, and this is explored below in a preliminary manner.

The effect of imperfection is investigated by repeating the non-linear finite element simulations on structures with a stochastic dispersion of nodal position. A MATLAB (Mathworks, 2002) routine is used to reposition randomly every finite element node of the structure. Since the ABAQUS finite element model uses five elements to describe each bar, the MATLAB routine introduces two types of imperfection: bar waviness and a misalignment of the bar joints. The magnitude of the random nodal displacement was chosen to be one third and two thirds of the bar radius. Predictions for a single stochastic realisation of each structure are given in Fig. 10c for the elastic–perfectly plastic material response. The figure gives the actuation load versus strain response of the *91hex-15%-P* KDLG with selected values of stockiness ($S = 0.001, 0.007$ and 0.025).

In all cases the presence of imperfections reduces the actuation stiffness. Since the most slender structure ($S = 0.001$) buckles in a symmetric elastic manner, imperfections give a negligible knockdown upon the buckling load and post-buckling (elastic) response. In contrast, the optimal structure ($S = 0.007$) and the stocky structure ($S = 0.025$) are imperfection sensitive. It is noted that the actuation strain corresponding to peak load is only mildly sensitive to imperfection in view of the fact that the actuation stiffness degrades with increasing imperfection. In the companion paper of this study (Symons et al., 2004), a more complete study is made

of the role of bar waviness and joint misalignment upon the actuation stiffness, and comparisons are made with manufactured structures.

6.3. Effect of shape of bar cross-section upon achievable actuation strain

The actuation performance of the modified KDLG can be improved somewhat with a change in bar cross-section from that of a solid circular bar to a hollow circular tube. For a bar of solid circular cross-section the radius of gyration is given by

$$\lambda = D/4. \tag{15}$$

Now consider a circular hollow cross-section bar of outer diameter D and inner diameter αD. The radius of gyration for this section is given by

$$\lambda = \sqrt{\frac{1-\alpha^4}{1-\alpha^2}}\frac{D}{4}. \tag{16}$$

Thus the ratio λ/D is greater for a hollow tube than for a solid circular bar.

The effect of cross-sectional shape upon the achievable actuation strain is plotted in Fig. 11a against S for hollow tubes ($\alpha = 0.9$ and 0.5) and for the solid-bar case ($\alpha = 0$), all for the *91hex-15%P* KDLG with the choice $\varepsilon_y = 1\%$. In the elastic buckling regime, the actuation strain for buckling is independent of α. However, when the achievable actuation strain is dictated by the onset of yield, the hollow bar outperforms the solid cross-section. This can be explained by the following scaling argument. Assume that the actuation strain scales with the bar curvature, with yield dictated by bar bending. The non-dimensional curvature at yield of a circular

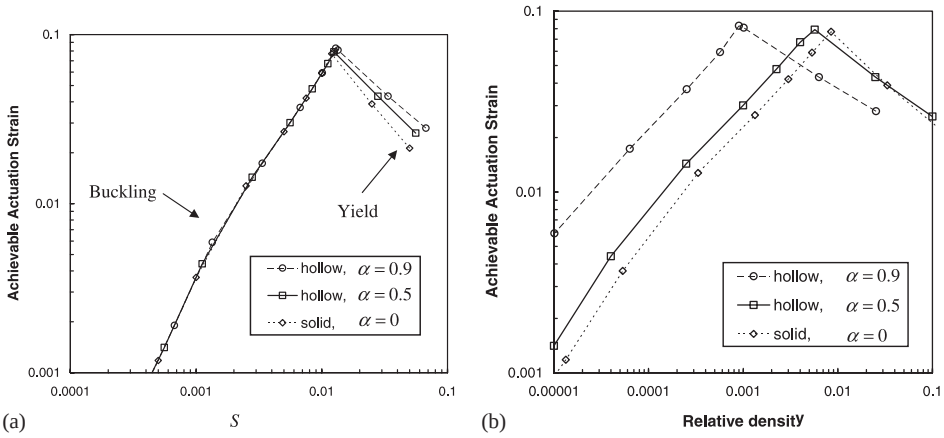

Fig. 11. (a) Achievable actuation strain (for $\varepsilon_y = 1\%$) for *91hex-15%-P* KDLG with solid or hollow bars as a function of stockiness and (b) as a function of relative density.

cross-section is

$$\kappa_y L = 2\varepsilon_y \frac{L}{D} = \frac{2\varepsilon_y}{S}\frac{\lambda}{D}. \tag{17}$$

It is evident from (16) that λ/D increases with increasing α and therefore, *for the same stockiness S,* a hollow bar has a greater curvature at yield than a solid bar.

The achievable actuation strain is replotted from Fig. 11a as a function of relative density of the structure in Fig. 11b. Here, relative density is defined as the ratio of the density of the structure, upon treating it as a smeared-out continuum, to the density of the solid material. The figure reveals that a KDLG constructed from hollow bars can accommodate higher actuation strains than a KDLG constructed from solid bars for a relative density below approximately 0.01 (with the choice $\varepsilon_y = 1\%$). At relative densities above 0.01 the order switches and solid bars are superior.

7. Concluding remarks

A statically and kinematically determinate, pin-jointed, double-layer grid has been developed, based upon the Kagome geometry. This structure contains no mechanisms or states of self-stress and is thereby an ideal topology for a morphing structure; it can resist externally applied loads yet can be internally actuated with minimal resistance. This double-layer grid also has a high bending stiffness as its faces comprise planar Kagome lattices. The rigid-jointed version inherits the properties of the pin-jointed version: it has high passive stiffness but can be actuated against a small internal resistance upon replacing a bar by an actuator. The achievable actuation strain, as limited by yield and buckling, has been explored as a function of bar stockiness and cross-sectional shape, and of the yield strain of the solid. It is shown that the achievable actuation strain attains a maximum value for an optimal value of bar stockiness due to the competition between buckling and yield. It is concluded that the Kagome Double-Layer Grid is a promising topology for a morphing material. This motivates the companion paper (Symons et al, 2004); in the follow-on study, KDLG structures are manufactured and the measured actuation performances are compared with predictions including the role of imperfections.

Acknowledgments

The authors are grateful for financial support from a DARPA grant on synthetic multi-functional materials and wish to thank Profs. A. G. Evans, J. W. Hutchinson and M. F. Ashby for helpful discussions.

References

Babuska, I., Szabo, B.A., 1982. On the rates of convergence of the finite element method. Int. J. Numer. Methods Eng. 18, 323–341.

Babuska, I., Szabo, B.A., Katz, I.N., 1981. The p-version of the finite element method. SIAM J. Numer. Anal. 18, 515–545.

Bendsøe, M.P., Sigmund, O., 2002. Topology Optimization: Theory, Methods and Applications. Springer, Berlin.

Calladine, C.R., 1978. Buckminster Fuller's "tensegrity" structures and Clerk Maxwell's rules for the construction of stiff frames. Int. J. Solids Struct. 14, 161–172.

dos Santos e Lucato, S.L., Wang, J., Maxwell, P., McMeeking, R.M., Evans, A.G., 2004. Design and demonstration of a high authority shape morphing structure. Int. J. Solids Struct. 41, 3521–3543.

Guest, S.D., Hutchinson, J.W., 2003. On the determinacy of repetitive structures. J. Mech. Phys. Solids 51, 383–391.

Hutchinson, R.G., 2004. Mechanics of lattice materials. Ph.D. Thesis, University of Cambridge.

Hutchinson, R.G., Wicks, N., Evans, A.G., Fleck, N.A., Hutchinson, J.W., 2003. Kagome plate structures for actuation. Int. J. Solids Struct 40, 6969–6980.

Hyun, S., Torquato, S., 2002. Optimal and manufacturable two-dimensional, Kagomé-like cellular solids. J. Mater. Res. 7, 137.

HKS, 2003. ABAQUS/Standard Version 6.3.1. Hibbit, Karlsson and Sorenson Inc., Providence, RI.

MathWorks, 2002. MATLAB Version 6.5. The MathWorks Inc., Natick, MA, USA.

Pellegrino, S., 1993. Structural computations with the singular value decomposition of the equilibrium matrix. Int. J. Solids Struct. 30, 3025–3035.

Pellegrino, S., Calladine, C.R., 1986. Matrix analysis of statically and kinematically indeterminate frameworks. Int. J. Solids Struct. 22, 409–428.

PTC, 2001. Pro/MECHANICA Version 23.3. Parametric Technology Corporation, Needham, MA.

Symons, D.D., Shieh, J., Fleck, N.A., 2004. Actuation of the Kagome double layer grid. Part 2: effect of imperfections on the measured and predicted actuation stiffness. J. Mech. Phys. Solids, in press, doi:10.1016/j.jmps.2005.02.008.

Wicks, N., Guest, S.D., 2004. Single member actuation in large repetitive truss structures. Int. J. Solids Struct. 41, 965–978.